Facile Synthesis of Nitrogen and Sulfur Codoped Carbon from Ionic Liquid as Metal-Free Catalyst for Oxygen Reduction Reaction

Yiyi She,[†] Zhouguang Lu,[‡] Meng Ni,[§] Li Li,[†] and Michael K. H. Leung*,[†]

[†]Ability R&D Energy Research Centre, School of Energy and Environment, City University of Hong Kong, G5702, 5/F, Academic 1, Hong Kong, China

[‡]Department of Materials Science and Engineering, South University of Science and Technology of China, Shenzhen, Guangdong, China

[§]Department of Building and Real Estate, The Hong Kong Polytechnic University, ZN713, South Tower, 7/F , Block Z, Hong Kong, China

Ⓢ *Supporting Information*

ABSTRACT: Developing metal-free catalysts for oxygen reduction reaction (ORR) is a great challenge in the development of fuel cells. Nitrogen and sulfur codoped carbon with remarkably high nitrogen content up to 13.00 at % was successfully fabricated by pyrolysis of homogeneous mixture of exfoliated graphitic flakes and ionic liquid 1-butyl-3-methylimidazolium bis(trifluoromethanesulfonyl)imide ([Bimi][Tf$_2$N]). The exfoliated graphite flakes served as a structure-directing substance as well as additional carbon source in the fabrication. It was demonstrated that the use of graphite flakes increased the nitrogen doping level, optimized the composition of active nitrogen configurations, and enlarged the specific surface area of the catalysts. Electrochemical characterizations revealed that the N and S codoped carbon fabricated by this method exhibited superior catalytic activities toward ORR under both acidic and alkaline conditions. Particularly in alkaline solution, the current catalyst compared favorably to the conventional 20 wt % Pt/C catalyst via four-electron transfer pathway with better ORR selectivity. The excellent catalytic activity was mainly ascribed to high nitrogen doping content, appropriate constitution of active nitrogen configurations, large specific surface area, and synergistic effect of N and S codoping.

KEYWORDS: oxygen reduction reaction, nitrogen and sulfur codoping, ionic liquid, metal-free catalyst
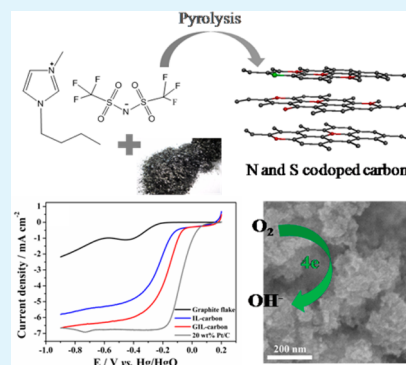
■ INTRODUCTION

Sluggish oxygen reduction reaction (ORR) kinetics and high cost of Pt-based catalysts are two major barriers that slow down the commercialization of fuel cells.[1] Over the past decades, significant effort has been devoted to explore Pt-free and even metal-free catalysts to improve catalytic activity and reduce cost.[2] Doped carbon, particularly N-doped carbon, has attracted increasing attention as a promising metal-free electrocatalyst for ORR due to its excellent electrocatalytic performance and low cost.[3] Recent studies have demonstrated that carbon materials monodoped or codoped by nonmetallic heteroatoms, such as N, S, P, and I, can achieve electrocatalytic activity comparable to Pt and exhibit superior selectivity and durability.[4−7] The mechanisms of the enhanced carbon catalysts are not yet clearly understood. For the N-doped carbon, some researchers explain that the metallic-like catalytic property results from the increase in electron density at the Fermi level, allowing the electrons to reach the conduction band.[8] Other study indicates that the insertion of N into graphitic matrix would create favorable positive sites for O$_2$ on the adjacent carbons owing to the electronegativity difference between N and C.[9] However, calculation based on density functional theory (DFT) shows that the excellent catalytic performance of N-doped carbon

materials is related to either the asymmetry spin density or atomic charge density, which may give new insight into the enhancement resulting from doping by heteroatoms (S, B, and P) whose electronegativity is no larger than C.[10] In the case of codoped carbon material, e.g., N and S codoped and N and P codoped,[6,11−14] synergetic effect also plays an important role in contributing to better performance when compared with monodoped carbon materials.

In recent years, intensive efforts have been contributed to exploring various dopants for fabricating doped carbon by pyrolytic method. Organic polymers and cyclic compounds, e.g., polyaniline, pyrrole, and benzyl disulfide, are widely adopted as heteroatom sources.[4,15,16] The disadvantage of these precursors lies in the large extent of decomposition or volatilization of organic compounds at high temperature, usually resulting in low heteroatom yields. Toxicity and unpleasant odor are other disadvantages. Ammonia is also used as N-containing dopant, but occupational safety and health issues are concerns.[17] Ionic liquids (ILs), which are

Scheme 1. Fabrication of N and S Codoped Carbon
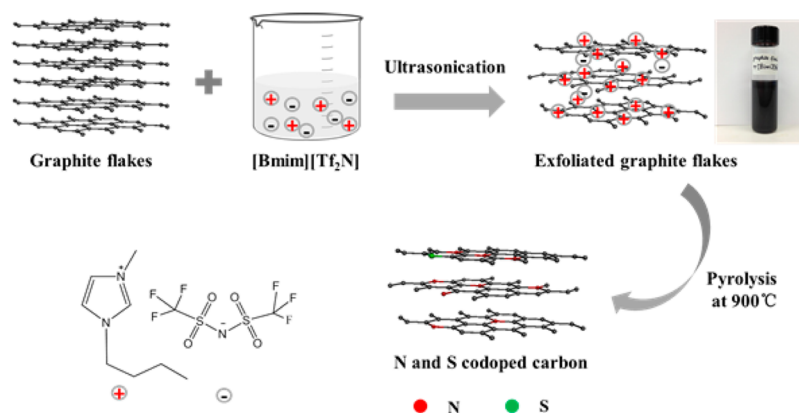
molten salts composed of ions, first attracted great interest in electrochemistry due to many superior properties such as high ion conductivity, negligible vapor pressure, high thermal stability, and wide varieties.[18] Recent interest in ILs has been directed to their use as precursors for fabricating doped carbon materials.[19] ILs are regarded as promising carbonization precursors for fabricating doped carbon materials with high doping content and tunable heteroatom composition.[20] N-doped carbon with N-doping content ranging from 5 to 14.2 wt % was successfully prepared by carbonization of ILs.[21−23] Dual-doped carbon materials, such as N, S codoped, N, B codoped, and N, P codoped, were also synthesized similarly with ILs containing more than one heteroatom.[24−26] However, ILs involving nitrile functional groups are selected in those cases because the nitrile groups can act as cross-linkable N sources, which are considered to be a prerequisite for synthesizing N-doped carbon by carbonization. Owing to the great prospect of these materials, conventional ILs without cross-linkable functional groups have also been explored for fabrication of heteroatom-doped carbon by introducing additional foreign frameworks although the carbon yield is relatively lower than that of nitrile-containing ILs. By being entrapped in carbon nanotubes matrix, conventional IL can be carbonized to doped carbon materials on the surface of carbon nanotubes, making it a fascinating core−shell microstructure.[27,28] It is also reported that silica gel has a confinement effect to ILs without nitrile group in carbonization, and thus can convert these ILs with negligible char residue into efficient carbon precursors.[29]

Herein, we report a successful fabrication of N and S codoped carbon by pyrolysis of a homogeneous mixture of exfoliated graphite flakes and conventional IL, 1-butyl-3-methyl-imidazolium bis(trifluoromethylsulfonyl)imide ([Bmim][Tf$_2$N]). The effects of exfoliated graphite flakes on the physiochemical properties of the as-prepared catalysts were studied in detail, which has not been published elsewhere to the best of our knowledge. Systematic investigation of the electrocatalytic performance of the as-prepared materials toward ORR in both acidic and alkaline conditions is also conducted. The exfoliated graphite flakes, or multilayer graphene, are simply prepared by ultrasonicating graphite flakes in [Bmim][Tf$_2$N].[30] In this process, the charged IL can be homogeneously absorbed on the exfoliated graphite flakes by electrostatic attraction, which prevents their restacking during pyrolysis. [Bmim][Tf$_2$N] can either go through confined carbonization within graphene framework or act as nitrogen and sulfur dopants for exfoliated graphite flakes.

Furthermore, since only graphite flakes and [Bmim][Tf$_2$N] are involved as precursors, no post-treatment of the pyrolytic products is necessary. That major ultrasonicating and pyrolysis processes are possible to be scaled up for mass production. The simplified and scalable fabrication process will significantly help promote the wide application of N and S codoped carbon catalyst.

■ EXPERIMENTAL SECTION

Sample Preparation. N and S codoped carbon was synthesized by pyrolysis of ultrasonicated mixture of graphite flakes and IL at 900 °C (Scheme 1). For comparison, the control sample without adding graphite flakes was also prepared under the same conditions. The samples fabricated with and without graphite flakes were labeled as GIL-carbon and IL-carbon, respectively. In a typical synthesis of GIL-carbon, 10 mg of graphite flakes (Sigma-Aldrich) was homogeneously dispersed in 2.5 mL of [Bmim][Tf$_2$N] (Sigma-Aldrich) by ultrasonication for 2 h. The suspension obtained was subsequently transferred to a corundum crucible and heated in a tube furnace at a heating rate of 5 °C min^{-1} to 900 °C. After holding this temperature for 1 h, the sample was allowed to cool to room temperature. All steps were carried out in a constant flow of N$_2$.

Characterization. The morphology and structure of the as-prepared catalysts were characterized by field emission scanning electron microscopy (FE-SEM, Hitachi S-4800) and transition electron microscopy (TEM, JEOL JEM 2100F). The surface chemical composition of each sample was analyzed by a PHI-5600 X-ray photoelectron spectroscopy (XPS) system with Mg Kα radiation ($h\nu$ = 1253.6 eV). Thermal gravimetric analysis (TGA) was carried out by a METTLER TOLEDO TGA/DSC 1 STAR^e System. The N$_2$ adsorption−desorption isotherms were recorded on Micromeritics ASAP 2020 analyzer at −196 °C (77 K). Prior to measurement, the samples were degassed at 250 °C under vacuum for 3 h. The specific surface area of GIL-carbon and IL-carbon was calculated by applying the Brunauer−Emmett−Teller (BET) model to the N$_2$ sorption data.

Electrochemical Measurements. All the electrochemical measurements were carried out in a three-electrode system connected to a CHI 660 electrochemical testing system. A commercial glassy carbon electrode (GCE, diameter of 5 mm, PINE instruments, U.S.A.) was used as the working electrode and a Pt foil as the counter electrode. A Hg/HgO (1 M KOH) electrode and a Ag/AgCl (3.5 M KCl) electrode were selected as the reference electrodes in alkaline and acidic conditions, respectively. For the rotating disk electrode (RDE) experiment, a PINE rotator was used. Prior to surface coating, the surface of GCE working electrode was polished in sequence with 1.0, 0.3, and 0.05 μm alumina powder on a polishing cloth and rinsed with deionized water. An amount of 10 μL suspension of as-prepared catalyst or graphite flakes or commercial Pt/C (20 wt % Pt/Vulcan XC-72 (Fuel Cell Earth LLC)) in anhydrous ethanol (1 mg sample mL^{-1}) was subsequently dropped onto the surface of the GCE with a

pipet and dried in air. This procedure was repeated three times. Finally, 10 μL of Nafion solution (0.5 wt %) was coated onto the surface of modified GCE and dried in air before use. All electrolytes were purged with high-purity O₂ or N₂ for 40 min prior to measurements. All the electrochemical experiments were performed at room temperature.

■ RESULTS AND DISCUSSION

The structure and morphology of the as-prepared GIL-carbon and IL-carbon were examined first. The typical SEM images (Figures 1a and 1b) clearly show that both GIL-carbon and IL-
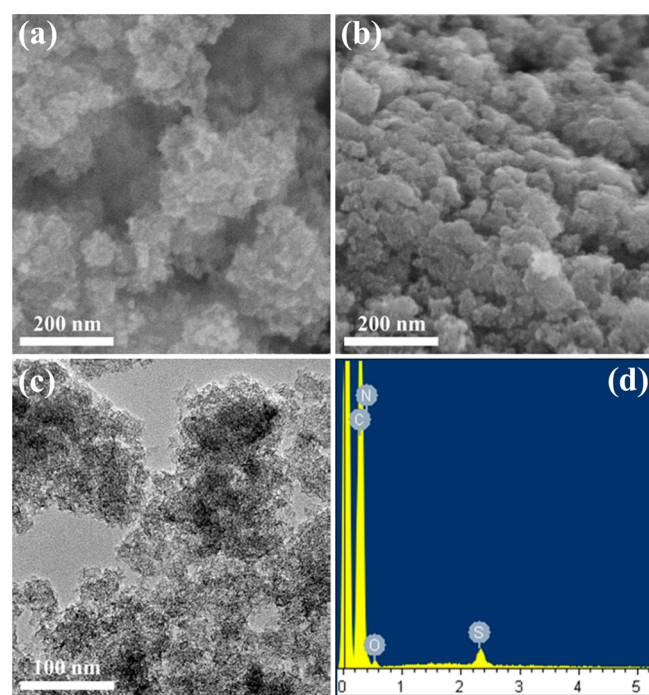

Figure 1. SEM images of (a) GIL-carbon and (b) IL-carbon; (c) TEM and (d) EDX of GIL-carbon.

Figure 2. Element mapping of GIL-carbon: (a) dark-field STEM image of the sample area on which mapping was carried out, (b) carbon map, (c) nitrogen map, and (d) sulfur map.

carbon are composed of small particle clusters, but the GIL-carbon has a looser structure compared with IL-carbon due to the confinement effects of exfoliated graphite flakes in the reactants. This structure is favorable for ORR because it facilies oxygen penetration and provides more active sites. Figure 1c presents the TEM image of the microstructure of GIL-carbon. The small particle clusters are actually composed of irregular thin flakes owing to the structure-directing effect of exfoliated graphite flakes. The EDX pattern of GIL-carbon shown in Figure 1d preliminarily reveals successful doping of a large quantity of N and small content of S into the carbon materials. The doping levels of N and S indicated by EDS are 13.02 and 0.44 at %, respectively. The element mapping images, as shown in Figure 2, clearly confirm the existence of N and S and also display the homogeneous distribution of the doped compositions.

The surface composition of N- and S-bonding configurations in the as-prepared samples was further investigated by XPS. The high-resolution N 1s and S 2p spectra of GIL-carbon and IL-carbon are shown in Figures 3a and 3b, respectively. The heteroatomic doping level and the percentage of each doping element are summarized in Table 1. According to Figure 3a, both N 1s spectra can be deconvoluted into four peaks, which correspond to pyridinic N (398.3 eV), pyrrolic N (399.7 eV),
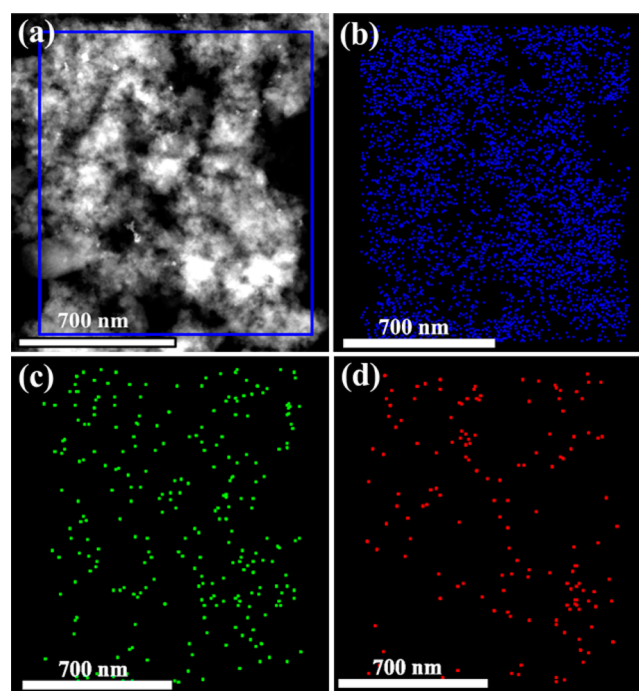
graphitic N (401.0 eV), and pyridinic N-oxide (403.4 eV).[17] However, the N-doping content in GIL-carbon reaches 13.00% with pyrodinic N and graphitic N contributing approximately equally, while the value in IL-carbon is only 9.88%, in which graphitic N dominates the N-doping by 43.4%. The higher N content of GIL-carbon proves the positive function of the exfoliated graphite flakes in the pyrolysis of IL [Bmim][Nf₂T]. The lower content of pyridinic N in IL-carbon can be ascribed to the fact that the [Bmim][Nf₂T] possesses no cross-linkage functional group such as cyano; thus, no pyridinic N can be formed from polymerization reaction.[31] It is suggested that the detected N species in char of IL-carbon exclusively results from the transformation of imidazole N in the precursor under high temperature.[32] On the other hand, the relatively high content of pyridinic N in GIL-carbon can be attributed to either the confined carbonization of [Bmim][Nf₂T] within exfoliated graphite flakes or the substitution of C atom with N in the framework of the few-layer graphene.[29] The actual pathway and mechanism still need to be further investigated. For the case of S, according to Figure 3b, the profound peaks located at 163.9 eV (−C−S−C−) and 165.0 eV (−C═S−) reveal successful S-doping although the contents in GIL-carbon and IL-carbon are 0.46% and 0.38%, respectively, which are much lower than that of N-doping.[33] The XPS results are consistent with the EDX measurements shown in Figure 1d.

Specific surface is considered to have profound effect on gas reaction like ORR.[34,35] N₂ adsorption−desorption isotherms of the as-prepared samples are presented in Figure 4. As expected, GIL-carbon exhibits a relatively larger BET surface area (503.6861 m² g⁻¹) than that of IL-carbon (413.5250 m² g⁻¹) due to the restacking prevention and the structure-directing effect of exfoliated graphite flakes. The increased BET surface area of GIL-carbon is believed to be beneficial to O₂ penetration and can provide more active sites for ORR.
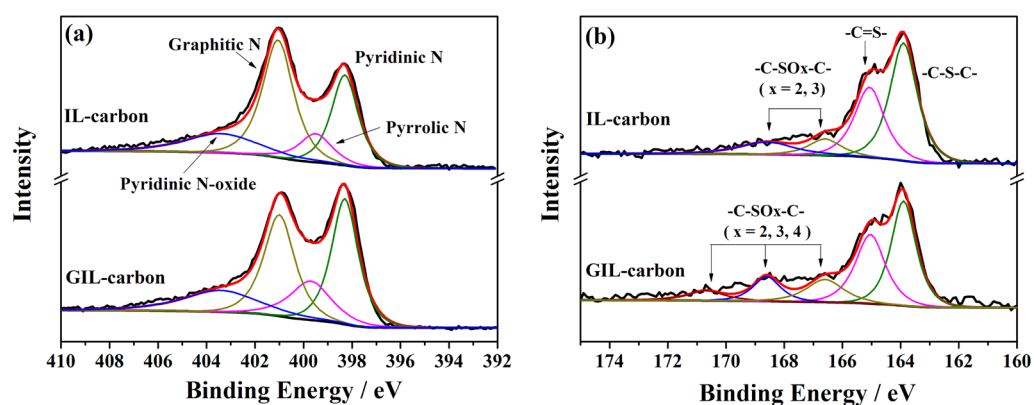
Figure 3. High-resolution XPS spectra of (a) N 1s and (b) S 2p in GIL-carbon and IL-carbon.

Table 1. Heteroatomic Doping Level and Peak Assignments for N 1s and S 2p from XPS Results

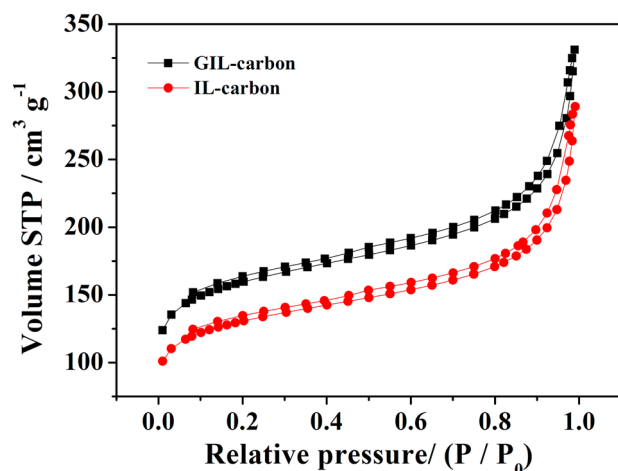| sample	N (at %)	N species (at %)			S (at %)	S species (at %)		
		pyridinic	pyrrolic	graphitic		C–SO$_x$-C	C=S	C–S–C
GIL-carbon	13.00	34.7	16.5	32.3	0.46	28.8	31.5	39.7
IL-carbon	9.88	28.9	11.2	43.4	0.38	18.5	32.1	49.4

Figure 4. N$_2$ adsorption−desorption isotherms of GIL-carbon and IL-carbon.

The electrocatalytic performance testing of the as-prepared samples was first conducted in alkaline condition. The results are presented in Figure 5 and Supporting Information Figure S3. Figure 5a exhibits the cyclic voltammograms (CVs) of the as-prepared catalysts for ORR compared with pristine graphite flakes and commercial 20 wt % Pt/C. Distinct peaks can be observed for both IL-carbon and GIL-carbon in the negative sweep, but the maximum current density of GIL-carbon is obviously larger than that of IL-carbon and is almost equal to that of 20 wt % Pt/C. Moreover, the peak potential of GIL-carbon is positive-shifted to −0.12 V (vs Hg/HgO) by adding exfoliated graphite flakes. The linear sweep voltammograms (LSVs) of these catalysts recorded by rotated disk electrode (RDE) in the same condition are plotted in Figure 5b. It can be seen that the LSV performance of GIL-carbon is better than that of IL-carbon with respect to both maximum current density and onset potential, which well agrees with the CVs observations. The maximum current density of GIL-carbon is comparable to the commercial Pt/C although the onset potential is still 0.15 V more negative than that of Pt, which

is comparable to the results of previous works.[14,36−38] Synergistic effect of N and S codoping is considered to play an important role in the activity enhancement of the as-prepared catalysts.[12] From the atomic point of view, both asymmetrical charge density and spin density are possible factors for an atom to serve as an active site with the latter being even more significant. The N-doping mainly influences the charge density owing to the different electronegativity between N and C. However, it was found that based on the DFT, the spin density of many atoms in the N and S codoped carbon materials, in addition to the charge density, was substantially uplifted due to the mismatch of the outermost orbitals of S and C.[39] This is also in accord with the good ORR catalytic activity of both IL-carbon and GIL-carbon. Further activity enhancement of GIL-carbon can be ascribed to the higher N-doping level, more active N configurations, and larger specific surface area. Actually, it is still unclear as to which type of doped N is the most active catalytic site toward ORR. Graphitic N is widely regarded as the most effective doped moiety because the positive-charge C atoms adjacent to doped N are theoretically more preferable to be absorbed by O$_2$ molecules.[17] However, N-doped carbon material containing only pyridinic and pyrrolic N also exhibits remarkable electrocatalytic activities toward ORR.[7] Therefore, based on the data obtained in this study, the excellent performance of GIL-carbon can be attributed to high N-doping content, appropriate constitution of active N configurations, large specific surface area, and synergistic effect of codoping with S.[40]

Concerning the practical application of GIL-carbon in fuel cells, its durability and tolerance to methanol in 0.1 M KOH were also investigated. During the chronoamperometric (CA) test, 3 M methanol was added after the test had run for 120 s. For the Pt catalyst, as shown in Figure 5c, the direction of current response reverses immediately after adding methanol. The phenomenon indicates the occurrence of methanol electrooxidation under this potential. In contrast, no noticeable change is observed on the GIL-carbon electrode, suggesting that its excellent tolerance to methanol and superior selectivity for ORR compare to that of conventional Pt. Additionally, GIL-carbon exhibits excellent durability for ORR in alkaline
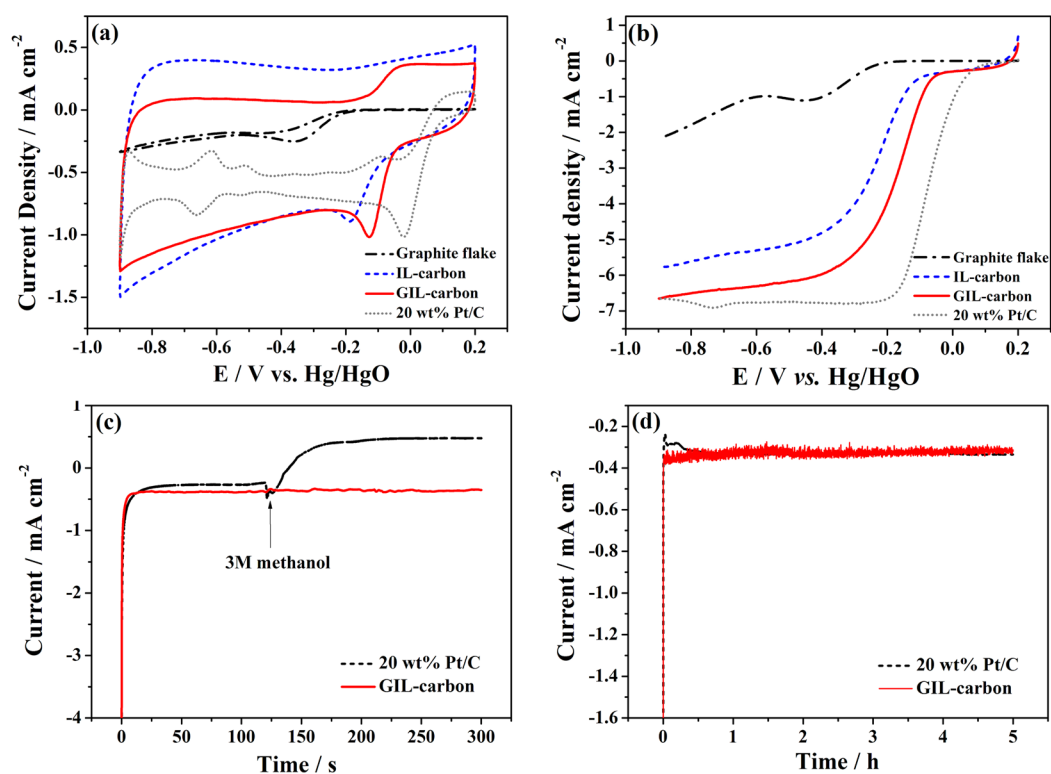
Figure 5. (a) Cyclic voltammograms and (b) RDE voltammograms (rotation rate: 2500 rpm) of different catalysts in O_2-saturated 0.1 M KOH solution at a scan rate of 10 mV s^{-1}; (c) chronoamperometric responses and (d) $I-t$ curves of GIL-carbon compared to 20 wt % Pt/C at -0.1 V (vs Hg/HgO) in O_2-saturated 0.1 M KOH solution.
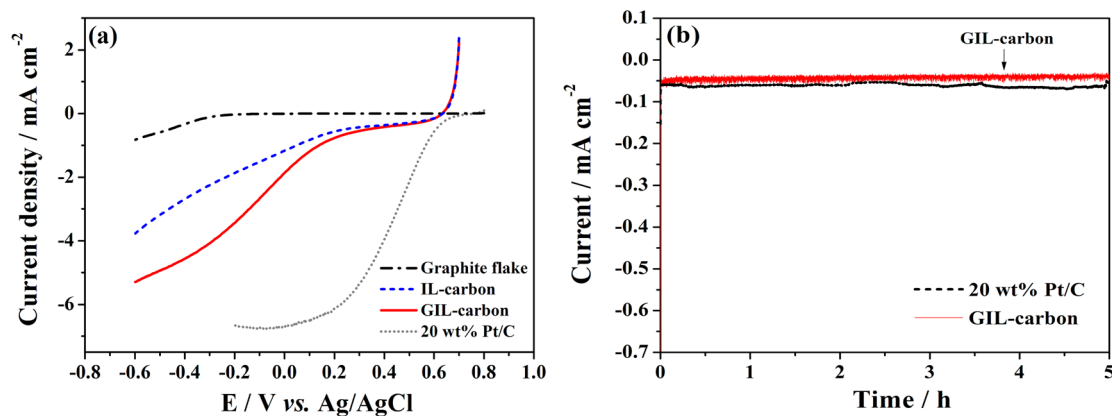

Figure 6. (a) RDE voltammograms (rotation rate: 2500 rpm) of different catalysts at a scan rate of 10 mV s^{-1} in O_2-saturated 0.1 M HClO$_4$ solution; (b) $I-t$ curves of GIL-carbon compared to 20 wt % Pt/C at -0.2 V (vs Ag/AgCl) in O_2-saturated 0.1 M HClO$_4$ solution.

condition as shown in Figure 5d. After continuous O_2 reduction for 5 h on the GIL-carbon electrode, the loss of current density is negligible, implying its potential application in alkaline fuel cells.

The electrocatalytic performances of GIL-carbon and IL-carbon were also studied in acidic condition. As shown in Figure 6a, both GIL-carbon and IL-carbon show obvious catalytic activity under acidic condition, and the maximum current density of GIL-carbon is still larger than that of IL-carbon just as the situation in alkaline environment. However, the ORR characteristic peaks shown at $-0.2\sim0.1$ V (vs Hg/HgO) in 0.1 M KOH no longer exist in 0.1 M HClO$_4$ solution (Supporting Information Figure S4). Therefore, the ORR catalytic activity of the as-prepared catalysts is inferior to that in alkaline condition. Moreover, the maximum current density of

GIL-carbon in 0.1 M HClO$_4$ is 5.2 mA cm^{-2}, which is smaller than 6.5 mA cm^{-2} in 0.1 M KOH solution. The lower catalytic activity in acidic condition is probably due to the significant decrease of disproportionation reaction of HO^{2-} into O_2 and OH$^-$, which is the electrocatalytic enhancement observed only by N-doped carbon materials.[41] It is worth noting that both maximum current density and onset potential of GIL-carbon are significantly improved compared with that of IL-carbon in acidic condition though it is still not as competitive as Pt. As can be seen in Figure 6b, a stable platform can be observed for GIL-carbon during the entire duration of the $I-t$ test, indicating its excellent durability for ORR in acidic condition.

To further probe the ORR kinetic process catalyzed by GIL-carbon, the number of electron transfer was studied based on the Koutecky–Levich equation[42]
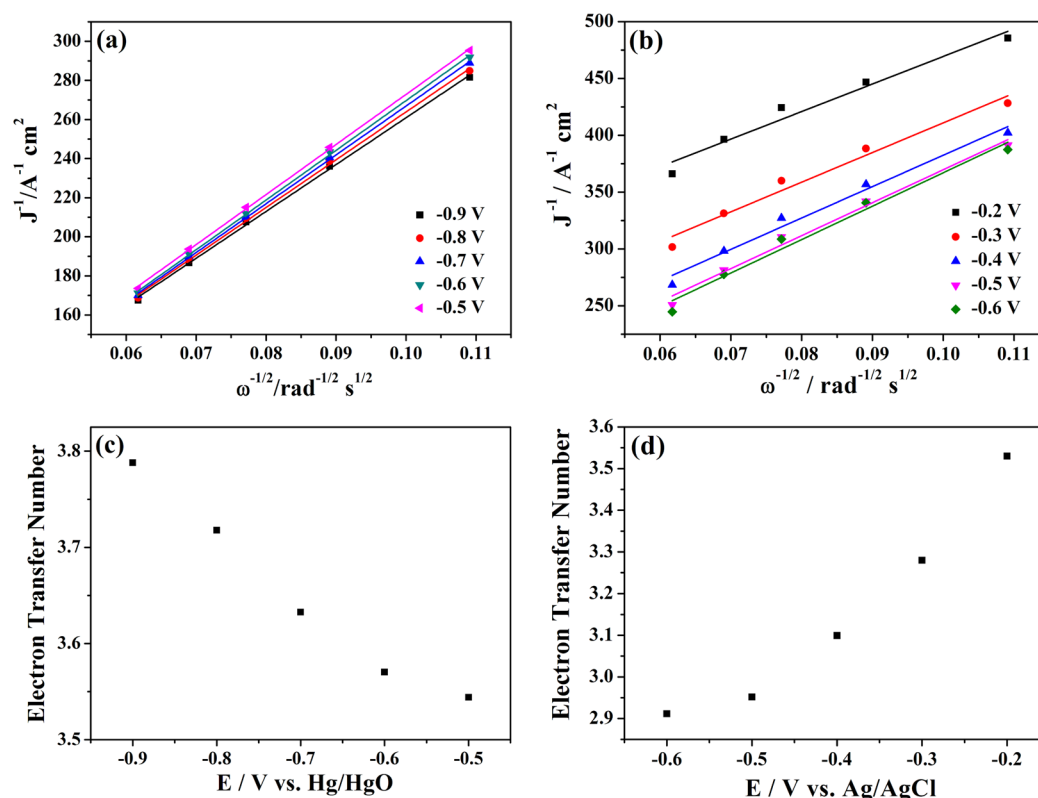
Figure 7. Koutecky−Levich plots at various voltages in (a) 0.1 M KOH and (b) 0.1 M HClO$_4$; electron transfer number determined by Koutecky−Levich plots at various voltages in (c) 0.1 M KOH and (d) 0.1 M HClO$_4$.

$$\frac{1}{j} = \frac{1}{j_k} + \frac{1}{j_d} = -\frac{1}{j_k} - \frac{1}{0.62nF(D_{O_2})^{2/3}v^{-1/6}C_{O_2}\omega^{1/2}}$$

where j is the measured current density; j_k and j_d are the kinetic and diffusion-limited current density, respectively; n is overall electron number transferred per oxygen molecule during ORR; F represents Faraday constant (96485 C mol^{-1}); D_{O2} is the diffusion coefficient of O$_2$ (1.9 × 10^{-5} cm^2 s^{-1} in 0.1 M KOH and 1.93 × 10^{-5} cm^2 s^{-1} in 0.1 M HClO$_4$);[43,44] ν is kinetic viscosity of the electrolyte (0.01 cm^2 s^{-1}); C_{O_2} is the bulk concentration of O$_2$ in the electrolyte (1.2 × 10^{-6} mol cm^{-3} in 0.1 M KOH and 1.26 × 10^{-6} mol cm^{-3} in 0.1 M HClO$_4$);[43,44] and ω is the electrode rotating rate (rad s^{-1}). Figure 7 displays the Koutecky−Levich plots of GIL-carbon at various voltages based on RDE voltammograms under different rotation rates (Supporting Information Figure S5) and the corresponding calculated electron transfer numbers in 0.1 M KOH and 0.1 M HClO$_4$. The Koutecky−Levich plots exhibit good linearity under plotted voltages in both alkaline (Figure 7a) and acidic (Figure 7b) conditions. According to Figure 7c, the ORR is regarded to go through a four-electron process in the entire voltage range in alkaline conditions although the electron transfer number slightly varies from 3.5 to 3.8. On the other hand, in acidic condition (Figure 7d), a mixture of four-electron and two-electron pathway is found on the GIL-carbon electrode for ORR during a large range of testing voltage, which is due to the fact that the active HO^{2-} intermediate is prone to receive a proton to form H$_2$O$_2$ in acidic environment. This is well consistent with the different CV and RDE performances of the GIL-carbon in acidic and alkaline conditions.

CONCLUSION

We have successfully fabricated nitrogen and sulfur codoped carbon with remarkably high N content by pyrolysis of homogeneous mixture of exfoliated graphite flakes and conventional ionic liquid [Bmim][Nf$_2$T]. The use of exfoliated graphite flakes increases the nitrogen doping level, optimizes the composition of active nitrogen configurations, and enlarges the specific surface area of the catalyst. The material prepared by this simple, economical, and scalable method possesses the properties of a superior metal-free electrocatalyst for oxygen reduction reaction in both alkaline and acidic conditions due to high nitrogen doping content, appropriate constitution of active nitrogen configuration, large specific surface area, and synergetic effect of nitrogen and sulfur codoping. Particularly in alkaline condition, the material exhibits comparable electrocatalytic activity to the commercial Pt catalysts with four-electron transfer pathway but a better ORR selectivity. Therefore, the N and S codoped carbon developed in this study shows great potential in electrochemical applications related to ORR such as alkaline fuel cells and metal air batteries.

ASSOCIATED CONTENT

Ⓢ Supporting Information

Effect of pyrolysis temperature; TGA profiles of GIL-carbon and IL-carbon; comparison of CVs of different catalysts in N$_2$-saturared and O$_2$-saturated conditions; CA responses of GIL-carbon in acidic conditions,; RDE voltammograms of GIL-carbon under various rotation rates. This material is available free of charge via the Internet at http://pubs.acs.org.

■ AUTHOR INFORMATION

Corresponding Author

*E-mail: mkh.leung@cityu.edu.hk. Fax: +852 3442 0688. Tel.: +852 3442 4626.

Notes

The authors declare no competing financial interest.

■ ACKNOWLEDGMENTS

■ REFERENCES

(1) Wu, J.; Yang, H. Platinum-Based Oxygen Reduction Electrocatalysts. *Acc. Chem. Res.* **2013**, *46*, 1848−1857.

(2) Chen, Z. W.; Higgins, D.; Yu, A. P.; Zhang, L.; Zhang, J. J. A Review on Non-Precious Metal Electrocatalysts for Pem Fuel Cells. *Energy Environ. Sci.* **2011**, *4*, 3167−3192.

(3) Yang, Z.; Nie, H.; Chen, X.; Chen, X.; Huang, S. Recent Progress in Doped Carbon Nanomaterials as Effective Cathode Catalysts for Fuel Cell Oxygen Reduction Reaction. *J. Power Sources* **2013**, *236*, 238−249.

(4) Yang, Z.; Yao, Z.; Li, G.; Fang, G.; Nie, H.; Liu, Z.; Zhou, X.; Chen, X.; Huang, S. Sulfur-Doped Graphene as an Efficient Metal-Free Cathode Catalyst for Oxygen Reduction. *ACS Nano* **2012**, *6*, 205−211.

(5) Yao, Z.; Nie, H.; Yang, Z.; Zhou, X.; Liu, Z.; Huang, S. Catalyst-Free Synthesis of Iodine-Doped Graphene via a Facile Thermal Annealing Process and Its Use for Electrocatalytic Oxygen Reduction in an Alkaline Medium. *Chem. Commun.* **2012**, *48*, 1027−1029.

(6) Yu, D.; Xue, Y.; Dai, L. Vertically Aligned Carbon Nanotube Arrays Co-Doped with Phosphorus and Nitrogen as Efficient Metal-Free Electrocatalysts for Oxygen Reduction. *J. Phys. Chem. Lett.* **2012**, *3*, 2863−2870.

(7) Li, Y.; Zhou, W.; Wang, H.; Xie, L.; Liang, Y.; Wei, F.; Idrobo, J.-C.; Pennycook, S. J.; Dai, H. An Oxygen Reduction Electrocatalyst Based on Carbon Nanotube−Graphene Complexes. *Nat. Nanotechnol.* **2012**, *7*, 394−400.

(8) Wong, W. Y.; Daud, W. R. W.; Mohamad, A. B.; Kadhum, A. A. H.; Majlan, E. H.; Loh, K. S. Nitrogen-Containing Carbon Nanotubes as Cathodic Catalysts for Proton Exchange Membrane Fuel Cells. *Diamond Relat. Mater.* **2012**, *22*, 12−22.

(9) Gong, K.; Du, F.; Xia, Z.; Durstock, M.; Dai, L. Nitrogen-Doped Carbon Nanotube Arrays with High Electrocatalytic Activity for Oxygen Reduction. *Science* **2009**, *323*, 760−764.

(10) Zhang, L.; Xia, Z. Mechanisms of Oxygen Reduction Reaction on Nitrogen-Doped Graphene for Fuel Cells. *J. Phys. Chem. C* **2011**, *115*, 11170−11176.

(11) Xu, J.; Dong, G.; Jin, C.; Huang, M.; Guan, L. Sulfur and Nitrogen Co-Doped, Few-Layered Graphene Oxide as a Highly Efficient Electrocatalyst for the Oxygen-Reduction Reaction. *ChemSusChem* **2013**, *6*, 493−499.

(12) Liu, Z.; Nie, H.; Yang, Z.; Zhang, J.; Jin, Z.; Lu, Y.; Xiao, Z.; Huang, S. Sulfur-Nitrogen Co-Doped Three-Dimensional Carbon Foams with Hierarchical Pore Structures as Efficient Metal-Free Electrocatalysts for Oxygen Reduction Reactions. *Nanoscale* **2013**, *5*, 3283−3288.

(13) Shi, Q.; Peng, F.; Liao, S.; Wang, H.; Yu, H.; Liu, Z.; Zhang, B.; Su, D. Sulfur and Nitrogen Co-Doped Carbon Nanotubes for Enhancing Electrochemical Oxygen Reduction Activity in Acidic and Alkaline Media. *J. Mater. Chem. A* **2013**, *1*, 14853−14857.

(14) Ai, W.; Luo, Z.; Jiang, J.; Zhu, J.; Du, Z.; Fan, Z.; Xie, L.; Zhang, H.; Huang, W.; Yu, T. Nitrogen and Sulfur Codoped Graphene: Multifunctional Electrode Materials for High-Performance Li-Ion Batteries and Oxygen Reduction Reaction. *Adv. Mater.* **2014**, *26*, 6186−6192.

(15) Hou, L.; Lian, L.; Li, D.; Pang, G.; Li, J.; Zhang, X.; Xiong, S.; Yuan, C. Mesoporous N-Containing Carbon Nanosheets towards High-Performance Electrochemical Capacitors. *Carbon* **2013**, *64*, 141−149.

(16) Unni, S. M.; Devulapally, S.; Karjule, N.; Kurungot, S. Graphene Enriched with Pyrrolic Coordination of the Doped Nitrogen as an Efficient Metal-Free Electrocatalyst for Oxygen Reduction. *J. Mater. Chem.* **2012**, *22*, 23506−23513.

(17) Lai, L.; Potts, J. R.; Zhan, D.; Wang, L.; Poh, C. K.; Tang, C.; Gong, H.; Shen, Z.; Lin, J.; Ruoff, R. S. Exploration of the Active Center Structure of Nitrogen-Doped Graphene-Based Catalysts for Oxygen Reduction Reaction. *Energy Environ. Sci.* **2012**, *5*, 7936−7942.

(18) Armand, M.; Endres, F.; MacFarlane, D. R.; Ohno, H.; Scrosati, B. Ionic-Liquid Materials for the Electrochemical Challenges of the Future. *Nat. Mater.* **2009**, *8*, 621−629.

(19) Paraknowitsch, J. P.; Thomas, A. Functional Carbon Materials from Ionic Liquid Precursors. *Macromol. Chem. Phys.* **2012**, *213*, 1132−1145.

(20) Fellinger, T.-P.; Thomas, A.; Yuan, J.; Antonietti, M. 25th Anniversary Article: "Cooking Carbon with Salt": Carbon Materials and Carbonaceous Frameworks from Ionic Liquids and Poly(Ionic Liquid)s. *Adv. Mater.* **2013**, *25*, 5838−5855.

(21) Hasché, F.; Fellinger, T.-P.; Oezaslan, M.; Paraknowitsch, J. P.; Antonietti, M.; Strasser, P. Mesoporous Nitrogen Doped Carbon Supported Platinum PEM Fuel Cell Electrocatalyst Made from Ionic Liquids. *ChemCatChem.* **2012**, *4*, 479−483.

(22) Fechler, N.; Fellinger, T.-P.; Antonietti, M. Salt Templating: A Simple and Sustainable Pathway toward Highly Porous Functional Carbons from Ionic Liquids. *Adv. Mater.* **2013**, *25*, 75−79.

(23) Yang, W.; Fellinger, T.-P.; Antonietti, M. Efficient Metal-Free Oxygen Reduction in Alkaline Medium on High-Surface-Area Mesoporous Nitrogen-Doped Carbons Made from Ionic Liquids and Nucleobases. *J. Am. Chem. Soc.* **2011**, *133*, 206−209.

(24) Fulvio, P. F.; Lee, J. S.; Mayes, R. T.; Wang, X.; Mahurin, S. M.; Dai, S. Boron and Nitrogen-Rich Carbons from Ionic Liquid Precursors with Tailorable Surface Properties. *Phys. Chem. Chem. Phys.* **2011**, *13*, 13486−13491.

(25) Paraknowitsch, J. P.; Zhang, Y.; Wienert, B.; Thomas, A. Nitrogen- and Phosphorus-Co-Doped Carbons with Tunable Enhanced Surface Areas Promoted by the Doping Additives. *Chem. Commun.* **2013**, *49*, 1208−1210.

(26) Fechler, N.; Fellinger, T.-P.; Antonietti, M. One-Pot Synthesis of Nitrogen−Sulfur-Co-Doped Carbons with Tunable Composition Using a Simple Isothiocyanate Ionic Liquid. *J. Mater. Chem. A* **2013**, *1*, 14097−14102.

(27) Ding, Y.; Sun, X.; Zhang, L.; Mao, S.; Xie, Z.; Liu, Z.-W.; Su, D. S. Entrapping an Ionic Liquid with Nanocarbon: The Formation of a Tailorable and Functional Surface. *Angew. Chem., Int. Ed.* **2015**, *54*, 231−235.

(28) Sa, Y. J.; Park, C.; Jeong, H. Y.; Park, S.-H.; Lee, Z.; Kim, K. T.; Park, G.-G.; Joo, S. H. Carbon Nanotubes/Heteroatom-Doped Carbon Core−Sheath Nanostructures as Highly Active, Metal-Free Oxygen Reduction Electrocatalysts for Alkaline Fuel Cells. *Angew. Chem., Int. Ed.* **2014**, *53*, 4102−4106.

(29) Wang, X.; Dai, S. Ionic Liquids as Versatile Precursors for Functionalized Porous Carbon and Carbon-Oxide Composite Materials by Confined Carbonization. *Angew. Chem., Int. Ed.* **2010**, *49*, 6664−6668.

(30) Wang, X.; Fulvio, P. F.; Baker, G. A.; Veith, G. M.; Unocic, R. R.; Mahurin, S. M.; Chi, M.; Dai, S. Direct Exfoliation of Natural Graphite into Micrometre Size Few Layers Graphene Sheets Using Ionic Liquids. *Chem. Commun.* **2010**, *46*, 4487−4489.

(31) Lee, J. S.; Wang, X.; Luo, H.; Dai, S. Fluidic Carbon Precursors for Formation of Functional Carbon under Ambient Pressure Based on Ionic Liquids. *Adv. Mater.* **2010**, *22*, 1004−1007.

(32) Wohlgemuth, S. A.; White, R. J.; Willinger, M. G.; Titirici, M. M.; Antonietti, M. A One-Pot Hydrothermal Synthesis of Sulfur and

Nitrogen Doped Carbon Aerogels with Enhanced Electrocatalytic Activity in the Oxygen Reduction Reaction. *Green Chem.* **2012**, *14*, 1515−1523.

(33) Su, Y.; Zhang, Y.; Zhuang, X.; Li, S.; Wu, D.; Zhang, F.; Feng, X. Low-Temperature Synthesis of Nitrogen/Sulfur Co-Doped Three-Dimensional Graphene Frameworks as Efficient Metal-Free Electrocatalyst for Oxygen Reduction Reaction. *Carbon* **2013**, *62*, 296−301.

(34) He, W.; Jiang, C.; Wang, J.; Lu, L. High-Rate Oxygen Electroreduction over Graphitic-N Species Exposed on 3d Hierarchically Porous Nitrogen-Doped Carbons. *Angew. Chem., Int. Ed.* **2014**, *53*, 9503−9507.

(35) Biddinger, E. J.; Ozkan, U. S. Role of Graphitic Edge Plane Exposure in Carbon Nanostructures for Oxygen Reduction Reaction. *J. Phys. Chem. C* **2010**, *114*, 15306−15314.

(36) Wan, K.; Long, G. F.; Liu, M. Y.; Du, L.; Liang, Z. X.; Tsiakaras, P. Nitrogen-Doped Ordered Mesoporous Carbon: Synthesis and Active Sites for Electrocatalysis of Oxygen Reduction Reaction. *Appl. Catal., B* **2015**, *165*, 566−571.

(37) Ma, F.-X.; Wang, J.; Wang, F.-B.; Xia, X.-H. The Room Temperature Electrochemical Synthesis of N-Doped Graphene and Its Electrocatalytic Activity for Oxygen Reduction. *Chem. Commun.* **2015**, *51*, 1198−1201.

(38) Lim, K. H.; Kim, H. Nitrogen-Doped Carbon Catalysts Derived from Ionic Liquids in the Presence of Transition Metals for the Oxygen Reduction Reaction. *Appl. Catal., B* **2014**, *158−159*, 355−360.

(39) Liang, J.; Jiao, Y.; Jaroniec, M.; Qiao, S. Z. Sulfur and Nitrogen Dual-Doped Mesoporous Graphene Electrocatalyst for Oxygen Reduction with Synergistically Enhanced Performance. *Angew. Chem., Int. Ed.* **2012**, *51*, 11496−11500.

(40) Zhang, C.; Hao, R.; Liao, H.; Hou, Y. Synthesis of Amino-Functionalized Graphene as Metal-Free Catalyst and Exploration of the Roles of Various Nitrogen States in Oxygen Reduction Reaction. *Nano Energy* **2013**, *2*, 88−97.

(41) Wiggins-Camacho, J. D.; Stevenson, K. J. Mechanistic Discussion of the Oxygen Reduction Reaction at Nitrogen-Doped Carbon Nanotubes. *J. Phys. Chem. C* **2011**, *115*, 20002−20010.

(42) Yin, J.; Qiu, Y.; Yu, J. Porous Nitrogen-Doped Carbon Nanofibers as Highly Efficient Metal-Free Electrocatalyst for Oxygen Reduction Reaction. *J. Electroanal. Chem.* **2013**, *702*, 56−59.

(43) Wang, S.; Yu, D.; Dai, L. Polyelectrolyte Functionalized Carbon Nanotubes as Efficient Metal-Free Electrocatalysts for Oxygen Reduction. *J. Am. Chem. Soc.* **2011**, *133*, 5182−5185.

(44) Marković, N. M.; Gasteiger, H. A.; Grgur, B. N.; Ross, P. N. Oxygen Reduction Reaction on Pt(111): Effects of Bromide. *J. Electroanal. Chem.* **1999**, *467*, 157−163.